JOURNAL OF AGRICULTURAL AND FOOD CHEMISTRY

pubs.acs.org/JAFC

Article

Synthesis, Antibacterial Activity, and Mechanisms of Novel Indole Derivatives Containing Pyridinium Moieties

Hongde Li, Shang Wu, Xiong Yang, Hongfu He, Zengxue Wu, Baoan Song, and Runjiang Song*

Cite This: *J. Agric. Food Chem.* 2022, 70, 12341−12354

Read Online

ACCESS | Metrics & More | Article Recommendations | Supporting Information

ABSTRACT: The development of effective antibacterial agents equipped with novel action modes and unique skeletons starting from natural compounds serves as an important strategy in the modern pesticide industry. Disclosed here are a series of novel indole derivatives containing pyridinium moieties and their antibacterial activity evaluation against two prevalent phytopathogenic bacteria, *Xanthomonas oryzae* pv. *oryzicola* (*Xoc*) and *X. oryzae* pv. *oryzae* (*Xoo*). A three-dimensional (3D)-QSAR model was adopted to discover higher activity like title compounds based on the *Xoc* antibacterial activity of the tested compounds. Compound **43** was consequently designed, and it displayed higher antibacterial activity as expected with the half-maximal effective concentration EC_{50} values of 1.0 and 1.9 μg/mL for *Xoo* and *Xoc*, respectively, which were better than those of the commercial drug thiodiazole copper (TC) (72.9 and 87.5 μg/mL). Under greenhouse conditions, the results of a rice *in vivo* pot experiment indicated that the protective and curative activities of compound **43** against rice bacterial leaf streak (BLS) and rice bacterial blight (BLB) were 45.0 and 44.0% and 42.0 and 39.3%, respectively, which were better than those of the commercial agent thiodiazole copper (38.0 and 37.9%, 38.6 and 37.0%) as well. Scanning electron microscopy images, defense enzyme activity tests, and proteomic techniques were utilized in a preliminary mechanism study, suggesting that compound **43** shall modulate and interfere with the physiological processes and functions of pathogenic bacteria.

KEYWORDS: *indole, pyridinium-containing, antibacterial activity, defense enzymes, antibacterial mechanisms*

INTRODUCTION

To date, plant bacterial and fungal diseases have always been the major enemies threatening world agricultural production, especially plant bacterial diseases such as rice bacterial blight (BLB) caused by *Xanthomonas oryzae pv. oryzae* (*Xoo*) and bacterial leaf streak (BLS) caused by *X. oryzae* pv. *oryzicola* (*Xoc*), which are two main pathogens spread in rice worldwide.[1] In general, an outbreak of BLB in rice would reduce rice production by 10−30%, reducing production by more than 50% or even failing to harvest.[2] As rice is infected with BLS, the yield is generally reduced by 10−20%, and this reduction can reach 40% in severe cases.[3] Significantly, rice is also an essential staple food as widely consumed over the world, especially in Asia and Africa.[4] Thus, prevention and control of rice bacterial diseases are urgent and are of critical importance to global agricultural security. Currently, available traditional antibacterial agents such as bismerthiazol,[5] thiodiazole copper, and agricultural streptomycin[6,7] still occupy the mainstream for controlling BLB and BLS. However, with the constantly evolving resistance to these agents,[8,9] a gradually increasing dosage is required to achieve the expected effect, which leads to extra costs and environmental pollution. Therefore, there remains an urgent need for the development of novel green antibacterial agents with cheap synthesis routes, powerful effects, and lower toxicity in the field of pesticide science.

Indole is one of the most common heterocycles in nature. Structurally, indole comprises the bicycle fusion of benzene and pyrrole rings, hence the aromaticity. In addition, its derivates have displayed versatile ability in many fields attributed to their physicochemical properties and bioactivities. As a representative example, indole has pleasing odors at low concentrations and has been widely applied as an additive in food and perfume production.[10] Some analogues derived from indole possess a broad spectrum of biological activities, including bactericidal,[11−16] fungicidal,[17−20] anticancer,[21,22] antiviral, and insecticidal[23−25] activities as well (Figure 1a). The research on indole derivatives has consequently always been one of the hot spots in drug discovery and pesticide development, attracting considerable attention.[26,27] Nevertheless, though indoles have exhibited great potential in agrochemical development, there have been insufficient indole-containing commercial pesticides applied in the field to date. In this regard, more research on indole applications needs to be conducted.

Our laboratory is committed to addressing practical issues in agriculture by discovering novel green pesticide candidates from lead compounds. In our previous studies, a series of compounds containing pyridinium salt were constructed. Biological tests showed that most of the title compounds had good antibacterial activity against *Xoo*, *Xanthomonas axonopodis* pv. *citri* (*Xac*), and *Ralstonia solanacearum*,[28−30] especially the lead compound **A1** (Figure 1b), which showed considerable inhibition activities

Received: June 14, 2022
Revised: September 8, 2022
Accepted: September 12, 2022
Published: September 22, 2022

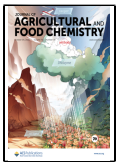

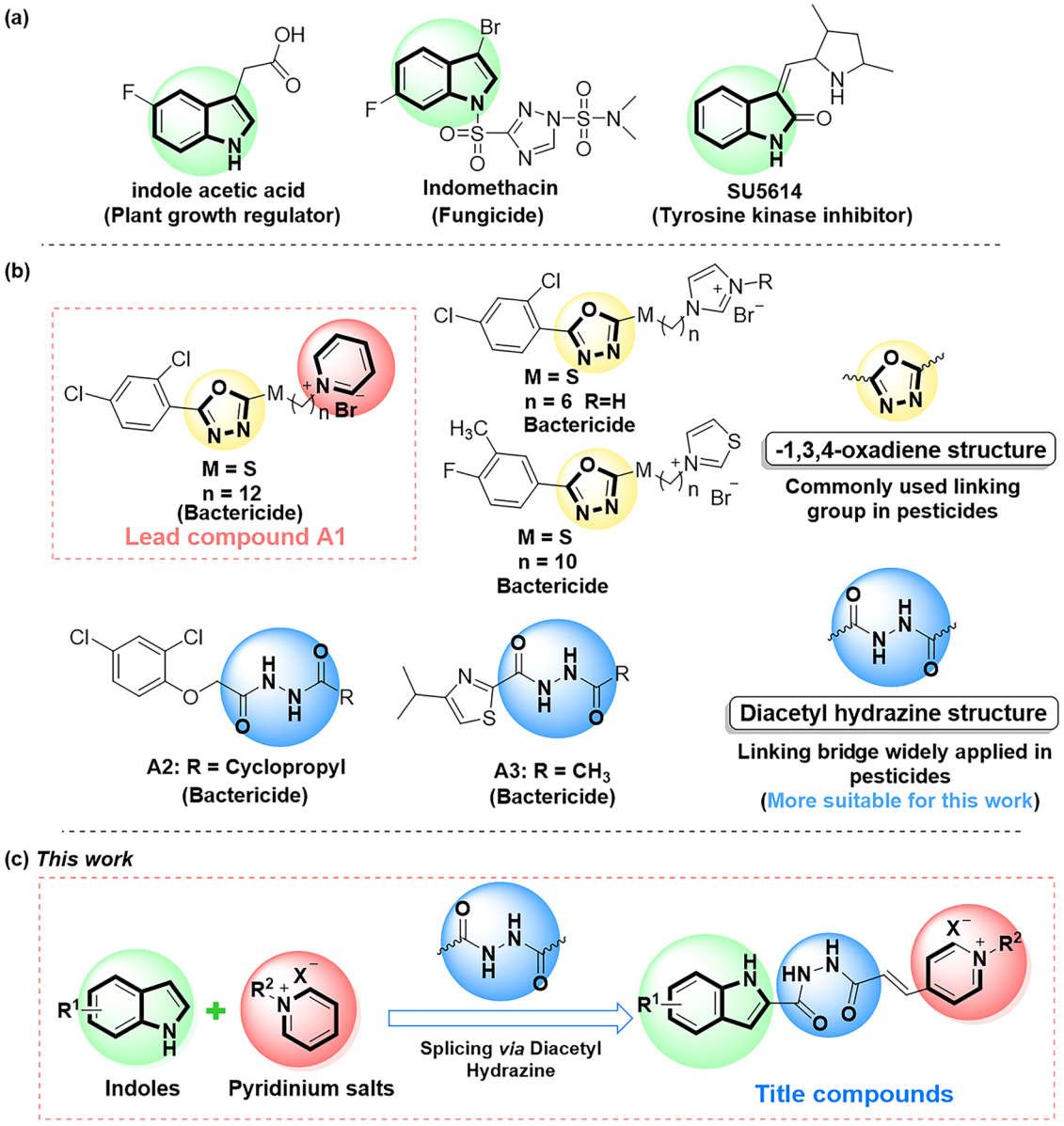

Figure 1. Natural indole derivatives with identified biological activities (a). Quaternary ammonium salt structure and diacetyl hydrazide structure derivatives with defined biological activity (b). Design of title compounds (c).

against phytopathogenic bacteria. Thus, the pyridinium salt behaved as the key functional backbone in antibacterial agents and could be employed as the active building block to introduce into other molecules. Additionally, the oxadiazole scaffold served as a significant bridge connecting to the benzene ring and pyridinium of the lead compound; this scaffold has proven antiplant bacterial activities and is a common bioactive skeleton in the construction of agrochemicals.[5,31] Meanwhile, as a ring-opening isostere of oxadiazole, diacetyl hydrazine usually served as a bioactive linkage between two functional groups, such as compounds **A2** and **A3** (Figure 1b).[32,33] We are interested in incorporating bioactive indole units into a pyridinium salt *via* oxadiazole or diacetyl hydrazine to access exciting antibacterial activity (Figure 1c). However, the connection between pyridinium and indole enabled by oxadiazole showed instability of title compounds in the early stage. In this case, diacetyl hydrazine was selected to be a better linkage. A double bond between diacetyl hydrazine and a pyridine ring provides molecules with a conjugated system, which further strengthens the structural stability, as active ingredients (AIs) in pesticides must be structurally stable so that they can remain effective under volatile conditions without being easily decomposed, resulting in a high durability of AIs.

Here, we disclosed a series of novel indole derivatives containing a pyridinium salt structure (Figure 2). Among these, title compound **43** exhibited excellent antibacterial activity against *Xoc* and *Xoo* through biological activity tests. We also conducted preliminary research on the antibacterial mechanism of the title compound **43**, involving the detection of the compound's defense enzymes against plants and related research on proteomics. Mechanistically, the related results suggested that these novel indole derivatives might display antibacterial activity through modulation and interference with pathogenic bacteria's physiological processes and functions.

MATERIALS AND METHODS

Chemicals. All reaction starting materials and some intermediates were purchased from Guizhou Hesheng Chemical Products Trading

https://doi.org/10.1021/acs.jafc.2c04213
J. Agric. Food Chem. 2022, 70, 12341−12354

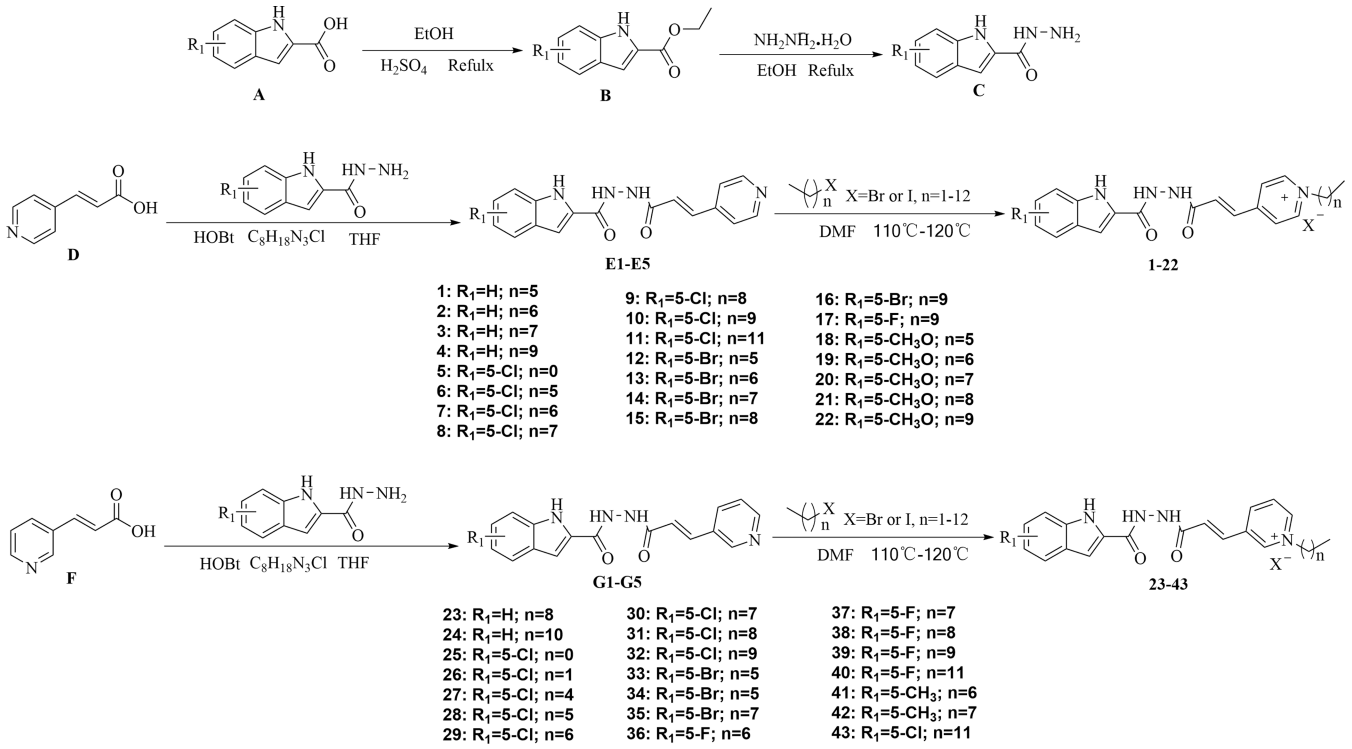

Figure 2. Synthesis route of the title compounds **1**−**43**.

Co., Ltd. (Guiyang, China), Guizhou Tongchuang Star Technology Co., Ltd. (Anshun, China), Shanghai McLean Biochemical Technology Co., Ltd. (Shanghai, China), and Shanghai Tengzhun Biotechnology Co., Ltd. (Shanghai, China). All solvents (≥98%) were purchased from Guizhou Zhongxing Chemical Materials Co., Ltd. (Guiyang, China).

Instrumental Analysis. The progress of the reaction was monitored by thin-layer chromatography on thin-layer silica gel GF_{254} (Shanghai Leigu Instrument Co., Ltd. Shanghai, China). Structural characterizations of all synthesized intermediates and title compounds were recorded on an EOL ECX-500 spectrometer (JEOL, Tokyo, Japan) and a Bruker Ascend-400 spectrometer (Bruker, Germany). High-resolution mass spectral (HRMS) data for all intermediates and title compounds were recorded on a Thermo Scientific Q Exactive (Thermo, USA). *In vitro* bioactivity tests and defense enzyme activity detection of compounds were performed using a Read Max 1900 microplate reader (Shanghai Flash Biotechnology Co., Ltd., China).

General Procedures for Preparation of Intermediates E1−E5. Intermediates **E1**−**E5** were prepared according to the reported method.[34] A mixture of 3 g of (*E*)-3-(pyridin-4-yl)acrylic acid (22.13 mmol) added to 1 mL of triethylamine was dissolved in 100 mL of tetrahydrofuran. Then, 4.24 g of EDCI (22.13 mmol), 3.37 g of HOBt (20.11 mmol), and 2-indolyl hydrazide with different substituents were added to the mixture. Refluxing the reaction by placing the reaction flask in an oil bath at 30 °C, the reaction system was monitored every 1 h. After 6 h of reaction, the raw materials in the system reacted completely, the reaction system was poured into a beaker, a large amount of water was added to the beaker, and the solid was precipitated by constant rotation and stirring. The precipitated solid was suction-filtered with a Buchner funnel. After the suction filtration was completed, it was dried under infrared conditions to obtain intermediates **E1**−**E5**.

General Procedures for Preparation of Intermediates G1−G5. Intermediates **G1**−**G5** were prepared according to the reported method.[34] A mixture of 2.5 g of 3-(3-pyridyl)acrylic acid (16.76 mmol) and 0.5 mL of triethylamine was dissolved in a 500 mL three-neck refluxing flask with tetrahydrofuran. Then, 3.86 g of EDCI (20.11 mmol), 3.06 g of HOBt (20.11 mmol), and 2-indolyl hydrazide with different substituents were added to the mixture. By placing the three-neck reaction flask in an oil bath and heating it to 30−40 °C for reflux reaction, the reaction system was monitored every 1 h. After 6 h of reaction, the raw materials in the system reacted completely; the reaction system was poured into a beaker, a large amount of water was added to the beaker, and the solid was precipitated by constant rotation and stirring. The precipitated solid was suction-filtered with a funnel. After the suction filtration was completed, it was dried under infrared conditions to obtain intermediates **G1**−**G5**.

General Procedures for Preparation of the Title Compounds (1−43). Intermediates **E1**−**E5** and **G1**−**G5** (1.14 mmol) were used as starting materials; brominated alkanes (2.29 mmol) with different chain lengths were dissolved in a three-neck reaction flask with 20 mL of DMF and gradually heated to 110−120 °C to start the reflux reaction for 6 h. After completion of the reaction and cooling, the desired product was filtered and further purified by recrystallization from methanol. The title compounds **1**−**43** were obtained. The yield of the title compounds was 32.70−65.29%, and the representative data for compound **1** are as follows. (*E*)-4-(3-(2-(1H-indole-2-carbonyl)-hydrazinyl)-3-oxoprop-1-en-1-yl)-1-hexylpyr-idin-1-ium bromide (1): yield: 47.59%; yellow solid; m.p. 255−256 °C; ^{1}H NMR (500 MHz, DMSO-d_6) δ 11.76 (s, 1H, −CH═CH−NH−), 10.72 (s, 1H, −CH═CH−CO−NH−), 10.66 (s, 1H, −NH−C−CO−NH−), 9.14 (d, J = 6.7 Hz, 2H, pyridyl-2-H + pyridyl-6-H), 8.37 (d, J = 6.7 Hz, 2H, pyridyl-3-H + pyridyl-5-H), 7.78 (d, J = 15.9 Hz, 1H, Indole-7-H), 7.67 (d, J = 8.0 Hz, 1H, Indole-4-H), 7.46 (d, J = 8.1 Hz, 1H, 3-(4-pyridyl)-CH═CH−), 7.32 (d, J = 15.9 Hz, 1H, Indole-3-H), 7.29 (d, J = 1.3 Hz, 1H, Indole-5-H), 7.22 (m, J = 11.6, 4.4 Hz, 1H, Indole-6-H), 7.07 (t, J = 7.5 Hz, 1H, 3-(4-pyridyl)-CH═CH−), 4.59 (t, J = 7.4 Hz, 2H, −N−CH_2−), 1.93 (m, 2H, −N−CH_2−CH_2−), 1.29 (m, 6H, (−CH_2−)$_3$$CH_3$), 0.87 (t, J = 6.7 Hz, 3H, −CH_2−CH_3). ^{13}C NMR (125 MHz, DMSO-d_6) δ 163.34 (s, 1C), 160.43 (s, 1C), 150.68 (s, 1C), 145.56 (s, 2C), 135.60 (s, 1C), 135.36 (s, 1C), 131.23 (s, 1C), 130.74 (s, 1C), 128.51 (s, 1C), 126.24 (s, 2C), 125.00 (s, 1C), 124.49 (s, 1C), 121.40 (s, 1C), 114.54 (s, 1C), 103.84 (s, 1C), 60.83 (s, 1C), 31.11 (s, 2C), 25.60 (s, 1C), 22.40 (s, 1C), 14.37 (s, 1C). HRMS (ESI): $C_{23}H_{27}O_2N_4BrNa$ [M + Na]$^+$ calcd for 493.12151, found 493.12079.

Antibacterial Activity *In Vitro*. *Xoo* and *Xoc* bacteria were inoculated on NA solid medium by the streaking method and cultured in a constant temperature incubator at 28 °C for about 1 week. A single

https://doi.org/10.1021/acs.jafc.2c04213
J. Agric. Food Chem. 2022, 70, 12341−12354

colony was taken from the NA solid medium, added to the NB liquid medium, and cultured to the logarithmic phase of growth. By referring to the relevant literature and making slight modifications to the method,[35] *in vitro* antimicrobial activity of all title compounds was assessed using a turbidimetric assay. A certain mass of the title compound to be tested was weighed, and it was dissolved in DMSO to prepare a certain concentration of the drug-containing mother solution. Then, a certain amount of the drug-containing mother solution was drawn into the NB liquid medium until the final concentration of the drug solution was 50 and 5 μg/mL, respectively; 50 μL of the bacterial suspension was grown to a logarithmic phase in the medium containing the drug and shaken in a constant temperature shaker at 28 °C and 180 rpm for 24−48 h until the medium of the CK treatment group grew to the log phase. The OD value (OD_{595}) of the bacterial solution of each treatment group was detected on a microplate reader. Sterilized water was the blank control, DMSO was the drug control, and the bacteriostatic activity of each drug was calculated after the OD value of the medium itself was corrected. The calculation formula of the inhibition rate is as follows

$$\text{inhibition rate } I(\%) = (C - T)/C \times 100$$

Based on the biological activity of the title compound in the preliminary screening, its EC_{50} value was calculated using software IBM SPSS Statistics 22.0 (SPSS, Chicago, IL). Each experiment was repeated three times.

3D-QSAR Analysis. Considering that these compounds show potent antibacterial effects, they have the potential to develop anti-*Xoc* and *Xoo* bacteria and promising application drugs. Comparative molecular field analysis (CoMFA) and comparative molecular similarity index analysis (CoMSIA) constructed three-dimensional (3D)-QSAR models were used to guide and describe the synthesis of small molecular compounds. Using SYBYL-X 2.1 software to build title compound molecules, the maximum repetitions (Max Iterations) were set to 10,000 and the stop criterion (Gradient) to 0.005, selecting the Tripos force field and Gasteiger-Huckel charge for molecular energy minimization. The most active compound **32** in the training set molecule form was selected as the template molecule, and the training set compound molecules were superimposed. CoMFA and CoMSIA calculation columns and compound pEC_{50} data were added with default settings in the superimposed training set molecule form, and the partial least-squares method was used to correlate the biological activity of the small molecule with its structural characteristics. First, the composition score was set to 10, the Leave-One-Out method was used to cross-validate the compounds in the training set, and then the composition score was modified to the best principal component score obtained by cross-validation for non-cross-validation regression calculation. The CoMFA and CoMSIA models built from the training set compounds were obtained. A conformational search method was used to optimize the model. Finally, the biological activities of the test set title compounds were predicted according to the constructed model.

Morphological Change. Morphological images of title compounds interacting with plant bacterial cells have been described in detail using scanning electron microscopy in our previously published paper.[36]

Antibacterial Activity *In Vivo*. Referring to the previous literature of the research group, with a slight modification,[37] the method of inoculating bacteria by cutting leaves was used to conduct the *in vivo* test of the title compound on BLB. Compound **43** and positive control drugs thiodiazole copper (TC, 20% suspending agent) were dissolved in DMSO and prepared with 0.2% Tween-80 solution at a concentration of 200 μg/mL; 90 mL of liquid medicine and water was sprayed on the rice leaves of the same growth until the droplets dripped. At 24 h after spraying, 2−3 cm was cut off from the tip of the rice leaf with a pair of scissors dipped in *Xoo* bacterial solution, treating 10−15 rice leaves with scissors on each healthy rice plant. The curative activity was evaluated similarly. On the first day, the scissors dipped in the bacteria solution was used to inoculate *Xoo* on the rice leaves by cutting the leaves and 10−15 rice leaves on each healthy rice plant were treated with the scissors. Then, 24 h after inoculation, the corresponding compound **43**, the positive control agent solution TC (20% suspending agent), and the negative control 0.2% Tween-80 solution were evenly sprayed on the rice leaves. The length of the disease spot of rice leaves was measured 14 days after the application, and the disease index and control effect were calculated according to the length of the disease spot.

According to the reference with a slight modification,[38] the pressure infiltration method was used to determine the curative and protective effects of compound **43** on BLS *in vivo* at a concentration of 200 μg/mL. To evaluate the protective activity of compound **43**, the title compound **43** and positive control agent TC (20% suspending agent) were dissolved in DMSO and diluted to a concentration of 200 μg/mL with 0.2% Tween-80 solution; 90 mL of the liquid medicine and water was sprayed on the rice leaves of the same growth until the droplets dripped. The negative control 0.2% Tween-80 solution and positive control TC (20% suspending agent) were operated according to the above method. After 24 h, at the 1/3 to 1/2 of the tip of the rice leaves, rice leaves were inoculated with a quantitative syringe containing *Xoc*. For curative activity, on the first day, the 1/3 to 1/2 of the tip of the rice leaves were infiltrated with a quantitative syringe containing *Xoc*. The title compound **43** and the positive control agents TC (20% suspending agent) were dissolved in DMSO and prepared with 0.2% Tween-80 solution at a concentration of 200 μg/mL; 90 mL of the liquid medicine and water was sprayed on the rice leaves of the same growth until the droplets dripped. Each treatment had 10−15 leaves and was repeated three times. The lesion length of rice leaves was measured on the 14th day after application, and the control effect was calculated according to the lesion length.

Determination of Defensive Enzyme Activities. When plants are stimulated by external physical, chemical, and biological factors, they will activate their own defense system and produce related defense enzymes to resist the influence of external adverse factors on themselves. The main function of superoxide dismutase (SOD) is to catalyze the disproportionation of superoxide anion free radicals into hydrogen peroxide and oxygen, and the superoxide anion free radicals produced are the normal metabolic products in living organisms. It is the most important free radical scavenger in the living body.[39] Peroxidase (POD) widely exists in various plant organs and different developmental stages and plays an important role in plant growth and under adversity.[40] Phenylalanine ammonia-lyase (PAL) is an inducible enzyme, and its content in plants can be used as a physiological indicator of plant disease resistance. Studies have shown that when plants are infected by pathogens, there will be an increase in the PAL activity in plants, accompanied by an increase in the amount of lignin synthesis.[41] Catalase (CAT), which exists in plant tissues in very large quantities, mainly decomposes hydrogen peroxide into oxygen and water, so that the plant body is protected from poisoning and thus increases the disease resistance of plants.[42] Therefore, we investigated the changes in defense enzymes such as CAT, PAL, SOD, and POD involved in the detection on the 1st, 3rd, 5th, and 7th days after infection of rice leaves with *Xoc* pathogens. Several healthy rice plants that had been planted in the greenhouse for 45 days were selected and the senescent yellow leaves of the healthy rice plants were cut off. The title compound **43** was dissolved in a 100 mL watering can, and the drug solution was diluted to a concentration of 200 μg/mL with 0.2% Tween-80 solution. The leaves were sprayed until the liquid dripped naturally. One day later, the leaves of healthy rice plants were infected with the *Xoc* pathogen using a quantitative syringe. Plants were treated with TC (20% suspending agent) and 0.2% Tween-80 solution as positive and negative controls, respectively. On the 1st, 3rd, 5th, and 7th days after the rice leaves were infected with the *Xoc* pathogen and after the batch collection of samples was completed, the enzyme kit of Suzhou Keming Biotechnology Co., Ltd. (100 tubes/96 samples, micro method) was used in the determination of defense enzyme activity in rice plants.

Label-Free Proteomics Analysis. Preparation of rice samples for proteomics. Greenhouse cultivation was selected to cultivate healthy rice plants at the stage of about 8−10 leaves. The title compound **43** was dissolved with dimethyl sulfoxide and then diluted with 0.2% Tween-80 to make the test solution of concentration 200 μg/mL and sprayed evenly on the leaves of rice until the liquid dripped naturally. 24 h after

https://doi.org/10.1021/acs.jafc.2c04213
J. Agric. Food Chem. 2022, 70, 12341−12354

Table 1. Antibacterial Activities of Compounds 1−43 against *Xoc In Vitro*

	inhibition (%)					
compd	50 μg/mL	5 μg/mL	regression equation	r	EC_{50} (μg/mL)[a]	95% confidence interval (μg/mL)
1	72.9 ± 1.3	22.5 ± 1.9	$y = 0.72x + 31.70$	0.95	16.6 ± 1.5	6.52−31.32
2	69.7 ± 1.1	29.4 ± 1.6	$y = 0.92x + 21.64$	0.99	14.9 ± 1.6	11.69−35.74
3	70.4 ± 0.4	15.1 ± 0.2	$y = 0.79x + 21.02$	0.96	23.8 ± 0.8	20.43−27.69
4	73.8 ± 0.7	15.8 ± 0.6	$y = 0.42x + 22.20$	0.96	41.9 ± 0.9	25.00−67.13
5	28.9 ± 1.7		$y = 0.30x + 10.25$	0.93	96.6 ± 0.9	6.70−1252.00
6	51.9 ± 1.6		$y = 0.35x + 26.32$	0.95	92.3 ± 1.0	53.92−149.27
7	73.0 ±1.8	18.9 ± 0.6	$y = 0.75x + 25.80$	0.95	79.8 ± 1.5	49.95−119.48
8	43.4 ± 1.1		$y = 0.37x + 20.76$	0.97	31.1 ± 1.3	25.23−38.25
9	68.4 ± 1.2	18.9 ± 0.7	$y = 0.75x + 25.64$	0.97	20.4 ± 1.8	9.92−37.45
10	71.9 ± 0.8	15.0 ± 1.1	$y = 0.79x + 23.03$	0.95	21.5 ± 2.0	14.20−31.53
11	71.9 ± 0.9	17.6 ± 0.7	$y = 0.77x + 26.79$	0.95	19.0 ± 1.3	9.34−33.83
12	53.3 ±1.7		$y = 1.49x + 25.34$	0.96	19.6 ± 1.4	9.97−34.46
13	69.3 ± 0.9	16.4 ± 1.3	$y = 0.82x + 21.27$	0.96	22.2 ± 1.9	12.35−38.09
14	71.2 ±1.3	22.0 ± 1.6	$y = 0.77x + 26.31$	0.97	19.4 ± 1.1	7.83−39.14
15	51.6 ± 1.4		$y = 0.77x + 25.98$	0.97	19.5 ± 1.6	8.42−38.09
16	100	99.2 ± 1.2	$y = 7.96x + 24.99$	0.97	3.4 ± 0.9	0.46−1.81
17	45.8 ± 0.8		$y = 0.54x + 13.92$	0.98	47.5 ± 0.9	10.75−172.31
18	45.8 ± 0.4		$y = 0.40x + 21.09$	0.95	45.3 ± 0.6	25.34−78.11
19	54.3 ± 0.6		$y = 0.38x + 27.65$	0.97	37.7 ± 1.5	11.20−86.04
20	67.7 ± 0.4	11.5 ± 0.7	$y = 1.28x + 30.03$	0.98	24.7 ± 1.0	21.18−28.83
21	70.9 ± 0.2	7.8 ± 0.6	$y = 1.41x + 25.43$	0.94	25.2 ± 0.8	21.74−29.28
22	70.6 ± 0.4	7.4 ± 0.7	$y = 1.32x + 35.80$	0.97	19.9 ± 0.7	9.34−37.69
23	99.9 ± 0.9	29.8 ± 1.7	$y = 0.84x + 21.92$	0.97	21.1 ± 1.4	9.73−41.68
24	74.9 ± 0.2	16.8 ± 0.9	$y = 0.87x + 17.65$	0.97	11.8 ± 0.7	6.86−20.48
25	24.1 ± 1.4		$y = 0.32x + 7.37$	0.99	49.9 ± 1.6	20.79−119.68
26	27.2 ± 1.9		$y = 0.31x + 8.84$	0.99	47.5 ± 1.1	23.34−94.52
27	30.8 ± 0.4		$y = 0.33x + 13.44$	0.99	53.4 ± 1.7	32.78−83.02
28	31.2 ± 1.0		$y = 0.34x + 12.17$	0.98	17.4 ± 1.8	11.44−32.73
29	70.7 ± 0.6	19.5 ± 1.2	$y = 0.80x + 24.10$	0.96	22.2 ± 1.8	9.63−37.90
30	97.6 ± 0.7	33.1 ± 1.0	$y = 1.61x + 23.18$	0.96	10.5 ± 2.1	6.47−16.24
31	97.8 ± 1.3	35.9 ± 1.1	$y = 1.55x + 25.36$	0.96	5.8 ± 0.8	0.41−15.92
32	98.1 ± 1.9	36.2 ± 1.1	$y = 1.54x + 26.34$	0.96	4.9 ± 1.3	0.13−17.97
33	66.1 ± 0.7	22.0 ± 1.9	$y = 0.75x + 25.34$	0.98	20.8 ± 1.5	7.70−46.06
34	97.2 ± 1.5	41.5 ± 1.8	$y = 0.73x + 28.24$	0.97	9.6 ± 1.7	4.22−17.38
35	98.2 ± 1.6	41.7 ± 0.6	$y = 0.75x + 28.94$	0.95	17.9 ± 1.2	9.16−30.44
36	74.1 ± 0.2	18.2 ± 0.6	$y = 1.16x + 39.60$	0.97	18.6 ± 0.5	15.79−21.74
37	72.6 ± 0.4	16.5 ± 1.7	$y = 1.29x + 35.68$	0.98	19.6 ± 0.4	11.41−31.34
38	65.9 ± 0.4	17.1 ± 0.6	$y = 1.44x + 28.16$	0.99	22.2 ± 0.5	5.97−66.62
39	97.8 ± 0.8	38.4 ± 0.9	$y = 1.62x + 25.50$	0.94	9.6 ± 1.6	5.94−14.57
40	96.3 ± 0.4	37.1 ± 0.5	$y = 1.57x + 22.71$	0.95	11.0 ± 1.2	6.16−18.87
41	46.9 ± 0.4		$y = 0.39x + 19.72$	0.96	49.9 ± 1.3	27.68−89.80
42	77.5 ± 0.3	15.4 ± 0.7	$y = 1.33x + 36.72$	0.95	18.7 ± 1.1	12.07−27.57
43	100	99.3 ± 0.2	$y = 6.96x + 29.01$	0.97	1.9 ± 0.7	0.97−3.27
I-12[b]	100	46.91 ± 0.1	$y = 5.78x + 29.89$	0.98	4.6 ± 0.6	2.12−9.48
TC[c]	34.7 ± 0.6		$y = 0.19x + 23.76$	0.99	87.5 ± 0.8	21.64−213.97

[a]Average of three replicates. [b]Lead compound reported by Wang et al.[29] [c]Commercial antibacterial agent (20%, suspending agent).

spraying, each healthy rice leaf was inoculated with the *Xoc* pathogen by osmosis using a dosing syringe. On the 3rd day after inoculation, all of the rice leaves inoculated with the *Xoc* pathogen were collected with a pair of scissors, and 3 g of rice leaf samples were weighed and snap-frozen in an −80 °C refrigerator. The methods of protein extraction and identification have been described in detail in our previous work.[43] Gene Ontology (GO) analysis includes cellular components (CCs), biological processes (BPs), and molecular biological functions (MFs). We performed GO analysis on the differential proteins of the CK + *Xoc* group and *Xoc* + **43** to clarify its antibacterial mechanism of action. Meanwhile, Kyoto Encyclopedia of Genes and Genomes (KEGG) annotations were performed using the KEGG pathway database (http://www.genome.jp/Pathway), which is conducive to an in-depth understanding of the biological functions of the proteins.

RESULTS AND DISCUSSION

Chemistry. As illustrated in Figure 2, using ethyl indole-2-carboxylate with different substituents (52.85 mmol) as the raw material and ethanol as the solvent, intermediate **C** was synthesized by the hydrazinolysis reaction at 120 °C. At room temperature, the condensation reaction of intermediate **C** with acrylic acid in tetrahydrofuran solution gave a series of intermediates **E1−E5** and **G1−G5**, and then the title compounds **1−43** were prepared by the *N*-alkylation reaction.

https://doi.org/10.1021/acs.jafc.2c04213
J. Agric. Food Chem. 2022, 70, 12341−12354

Table 2. Antibacterial Activities of Compounds 1−43 against *Xoo In Vitro*

	inhibition (%)					
compd	50 μg/mL	5 μg/mL	regression equation	*r*	EC_{50} (μg/mL)[a]	95% confidence interval (μg/mL)
1	98.2 ± 0.6	38.3 ± 0.5	$y = 1.58x + 25.06$	0.95	9.9 ± 1.0	5.50−16.49
2	99.7 ± 1.0	34.6 ± 0.5	$y = 1.58x + 26.50$	0.97	9.4 ± 0.7	4.08−17.91
3	50.4 ± 1.6	17.7 ± 1.2	$y = 0.80x + 11.40$	0.99	35.0 ± 2.2	12.35−243.73
4	54.2 ± 0.5		$y = 0.74x + 30.19$	0.96	38.5 ± 0.7	16.60−75.03
5	31.0 ± 1.4		$y = 0.26x + 20.96$	0.98	75.3 ± 1.3	34.26−136.50
6	67.3 ± 2.3	23.7 ± 1.9	$y = 0.73x + 26.40$	0.98	20.5 ± 1.4	9.80−37.76
7	70.9 ± 0.6	24.2 ± 0.9	$y = 0.72x + 30.18$	0.97	19.5 ± 0.9	7.36−41.18
8	72.6 ± 0.7	26.8 ± 1.1	$y = 0.75x + 27.46$	0.97	18.8 ± 0.6	7.34−38.01
9	73.1 ± 0.9	25.2 ± 1.1	$y = 0.76x + 28.12$	0.96	18.1 ± 1.2	7.15−35.84
10	74.8 ± 1.4	25.3 ± 1.6	$y = 0.74x + 30.42$	0.96	17.0 ± 1.2	7.32−30.96
11	75.7 ± 1.1	25.5 ± 1.1	$y = 0.74x + 31.17$	0.95	16.6 ± 0.8	7.30−29.08
12	57.2 ± 1.7		$y = 0.35x + 32.56$	0.96	32.6 ± 0.6	16.38−53.82
13	99.2 ± 0.2	36.9 ± 1.9	$y = 1.34x + 34.71$	0.98	10.3 ± 1.3	3.09−17.81
14	99.9 ± 0.1	41.2 ± 1.4	$y = 1.43x + 31.94$	0.97	8.2 ± 1.9	2.22−17.86
15	54.9 ± 1.0		$y = 0.32x + 32.19$	0.96	35.8 ± 2.0	29.34−42.92
16	52.8 ± 1.0		$y = 0.37x + 28.91$	0.96	36.0 ± 1.6	18.08−61.45
17	66.2 ± 0.3	7.9 ± 1.3	$y = 1.51x + 25.07$	0.99	25.1 ± 0.4	13.25−47.70
18	47.0 ± 0.4		$y = 0.44x + 16.03$	0.96	49.2 ± 1.0	23.01−104.39
19	73.6 ± 0.5	19.2 ± 0.7	$y = 1.36x + 34.51$	0.97	18.9 ± 0.6	9.63−32.79
20	98.6 ± 0.2	30.8 ± 1.5	$y = 1.70x + 14.36$	0.96	13.9 ± 0.5	3.25−80.75
21	100	96.3 ± 0.4	$y = 3.50x + 17.92$	0.94	5.8 ± 0.5	4.34−7.83
22	79.6 ± 0.3	19.9 ± 1.6	$y = 1.35x + 36.09$	0.96	18.0 ± 0.4	10.44−28.40
23	98.3 ± 0.3	27.6 ± 1.4	$y = 1.68x + 20.17$	0.97	10.6 ± 0.8	6.41−18.18
24	93.8 ± 2.1	43.8 ± 1.1	$y = 1.33x + 32.65$	0.95	8.9 ± 1.2	6.34−12.37
25	24.0 ± 1.3		$y = 0.31x + 6.51$	0.98	100.7 ± 1.6	51.24−189.21
26	25.6 ± 1.1		$y = 0.30x + 9.64$	0.98	94.1 ± 1.8	54.11−156.75
27	95.2 ± 0.2	21.4 ± 1.5	$y = 0.88x + 13.04$	0.96	27.8 ± 1.0	20.43−38.16
28	69.0 ± 0.1	14.3 ± 0.6	$y = 0.85x + 20.20$	0.97	23.8 ± 0.9	12.14−39.63
29	99.9 ± 0.1	99.2 ± 0.2	$y = 8.00x + 22.10$	0.98	2.2 ± 1.4	0.64−6.20
30	99.6 ± 0.5	24.9 ± 0.6	$y = 0.89x + 16.25$	0.97	12.2 ± 0.7	6.81−21.59
31	99.5 ± 1.4	99.1 ± 0.1	$y = 3.31x + 20.85$	0.97	5.6 ± 2.4	2.46−11.85
32	99.8 ± 0.1	49.3 ± 0.7	$y = 3.29x + 21.26$	0.97	5.5 ± 2.1	2.74−10.60
33	98.1 ± 0.4	37.4 ± 1.6	$y = 1.59x + 24.64$	0.95	10.1 ± 1.8	5.82−16.34
34	100	49.5 ± 0.8	$y = 3.32x + 21.07$	0.97	5.5 ± 1.3	2.48−11.43
35	99.9 ± 0.1	55.0 ± 0.9	$y = 3.22x + 25.47$	0.95	4.8 ± 1.4	2.63−8.14
36	95.3 ± 0.1	39.1 ± 1.5	$y = 1.46x + 28.77$	0.94	10.8 ± 0.8	0.66−1.57
37	96.9 ± 0.1	41.7 ± 1.3	$y = 1.54x + 18.87$	0.95	10.4 ± 0.4	5.60−11.27
38	63.1 ± 0.4		$y = 0.27x + 20.65$	0.96	37.1 ± 0.8	23.00−56.04
39	71.9 ± 0.4	9.6 ± 1.6	$y = 1.31x + 34.35$	0.97	21.4 ± 0.5	13.34−33.09
40	100	56.7 ± 1.0	$y = 7.91x + 26.35$	0.95	4.7 ± 0.6	2.41−8.20
41	97.5 ± 0.5	34.9 ± 0.7	$y = 1.60x + 19.94$	0.98	12.0 ± 0.4	4.61−30.20
42	100	36.1 ± 1.0	$y = 1.58x + 25.70$	0.96	9.7 ± 0.7	4.28−18.74
43	99.6 ± 0.2	98.8 ± 2.4	$y = 7.85x + 24.65$	0.96	1.0 ± 0.4	2.99−4.24
I-12[b]	100	65.3 ± 2.7	$y = 8.17x + 15.58$	0.98	2.8 ± 0.7	1.72−4.74
TC[c]	28.7 ± 1.2		$y = 0.43x + 8.28$	0.97	72.9 ± 2.3	31.50−135.97

[a]Average of three replicates. [b]Lead compound reported by Wang et al.[29] [c]Commercial antibacterial agent (20%, suspending agent).

Melting points, yields, and compound characterization data for all title compounds (**1**−**43**) are provided in Supporting Information I.

Antibacterial Activity *In Vitro*. According to the turbidity method in the National Standard, the designed and synthesized title compounds **1**−**43** were tested for *Xoc* and *Xoo* biological activities (Tables 1 and 2). When the concentration was 50 μg/mL, title compounds **16**, **23**, **30**, **31**, **32**, **34**, **35**, **39**, **40**, and **43** exhibited excellent antibacterial activity against *Xoc* bacteria, and the antibacterial rates were 100, 99.9, 97.6, 97.8, 98.1, 97.2, 98.2, 97.8, 96.3, and 100%, respectively. The EC_{50} values of these compounds against *Xoc* pathogens were 3.4, 21.1, 10.5, 5.8, 4.9, 9.6, 17.9, 9.6, 11.0, and 1.9 μg/mL, respectively, each of which was greater than that of the commercial drug TC (87.49 μg/mL). Particularly, with an EC_{50} value of 1.9 μg/mL for the title compound **43**, it was more effective than the lead compound **A1** (4.62 μg/mL) in controlling *Xoc*.

When the concentration was 50 μg/mL, most of the title compounds had a good bacteriostatic effect against the *Xoo* pathogen, and the inhibition rate reached more than 90%. Among them, the inhibition rates of title compounds **21**, **29**, **31**, and **43** were 96.3, 99.2, 99.1, and 98.8% at 5 μg/mL. To further verify their activity, the EC_{50} values of title compounds **14**, **21**, **29**, **31**, **32**, **34**, **35**, **40**, and **43** against *Xoo* were 8.2, 5.8, 2.2, 5.6,

https://doi.org/10.1021/acs.jafc.2c04213
J. Agric. Food Chem. 2022, 70, 12341−12354

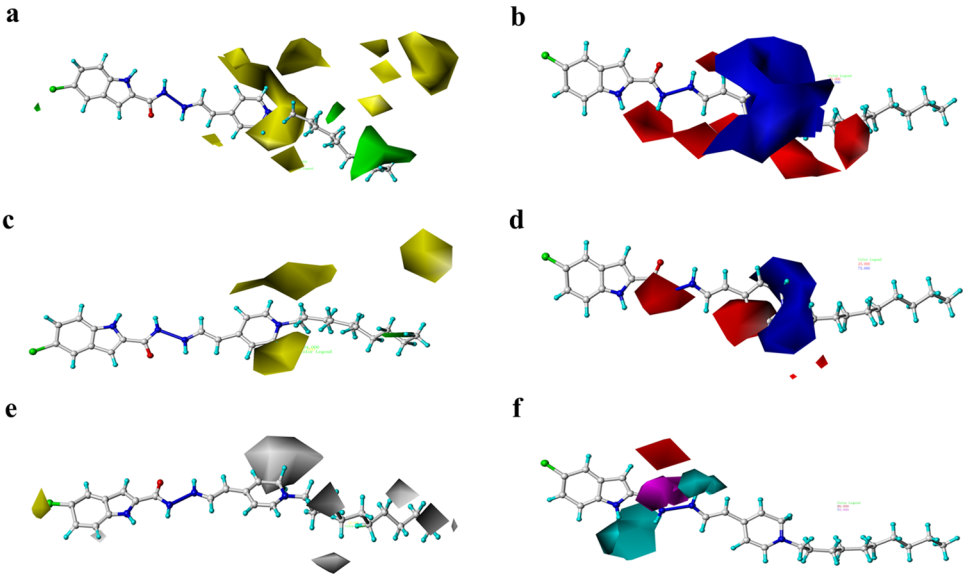

Figure 3. CoMFA contour maps of steric (a) and electrostatic (b) fields and CoMSIA contour maps of steric (c), electrostatic (d), hydrophobic (e), and H-bond acceptor (f) fields.

Table 3. Statistical Parameters of the CoMFA and CoMSIA Models

statistical parameter	CoMFA	CoMSIA	statistics reference threshold
q^2[a]	0.705	0.627	>0.5
ONC[b]	7	5	
r^2[c]	0.982	0.918	>0.8
SEE[d]	0.056	0.113	
F[e]	127.121	40.152	
fraction of field contributions			
steric	0.717	0.291	
electrostatic	0.283	0.252	
hydrophobic		0.357	
H-acceptor		0.036	
H-donor		0.064	

[a]Cross-validated correlation. [b]Optimum number of components. [c]Non-cross-validated correlation. [d]Standard error of the estimate. [e]Fisher statistics.

5.5, 5.5, 4.8, 4.7, and 1.0 μg/mL, respectively. These results were relatively superior to the commercial drug TC (72.9 μg/mL), of which the optimal compound **43** possessed a more potent effect in controlling *Xoo* than the lead compound **A1** (2.8 μg/mL) (Figure 3).

Table 4. Protective and Curative Activities *In Vivo* of Compound 43 against Rice Bacterial Leaf Blight under Greenhouse Conditions at 200 μg/mL[a]

	14 days after spraying				
treatment	morbidity (%)	disease index (%)[b]	protective activity (%)[c]	disease index (%)[b]	curative activity (%)[c]
43	100	50.8	42.0 ± 1.9*a*	53.5	39.3 ± 2.4*a*
TC	100	54.1	38.6 ± 1.9*b*	54.8	37.0 ± 2.0*b*
CK	100	87.6		86.7	

[a]All results are expressed as mean ± SD. [b]Disease index, which is a comprehensive indicator of the overall incidence and severity. [c]Statistical analysis was performed by analysis of variance (ANOVA) in SPSS 22.0 software with equal variances assumed (P > 0.05). The different lowercase letters indicate curative activity with different treatment groups at P < 0.05.

3D-QSAR Analysis. To make a 3D structure−activity relationship, the statistical parameters obtained are displayed in Table 3. After we superimposed the molecules, we established a database of align.mdb, and used the molecular spreadsheet and autofill functions to add COMFA and the derivative value of the inhibition rate. Using the PLS box in QSAR to use cross-

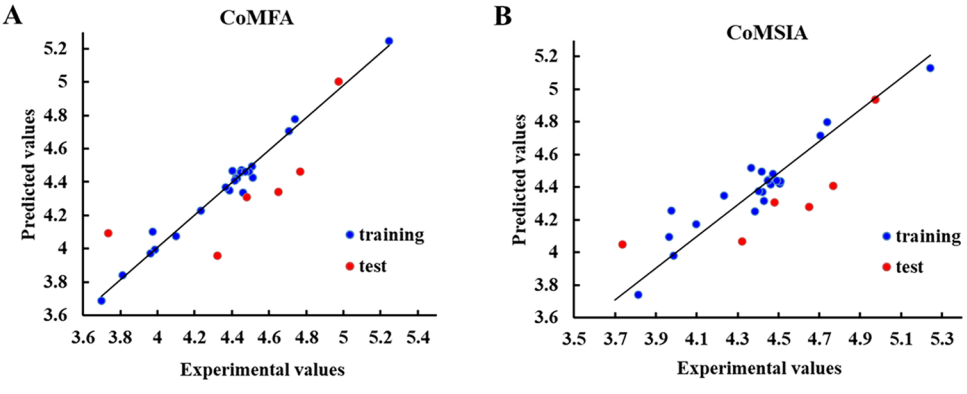

Figure 4. Plots of experimental and predicted pEC_{50} for the (A) CoMFA and (B) CoMSIA models.

https://doi.org/10.1021/acs.jafc.2c04213
J. Agric. Food Chem. 2022, 70, 12341−12354

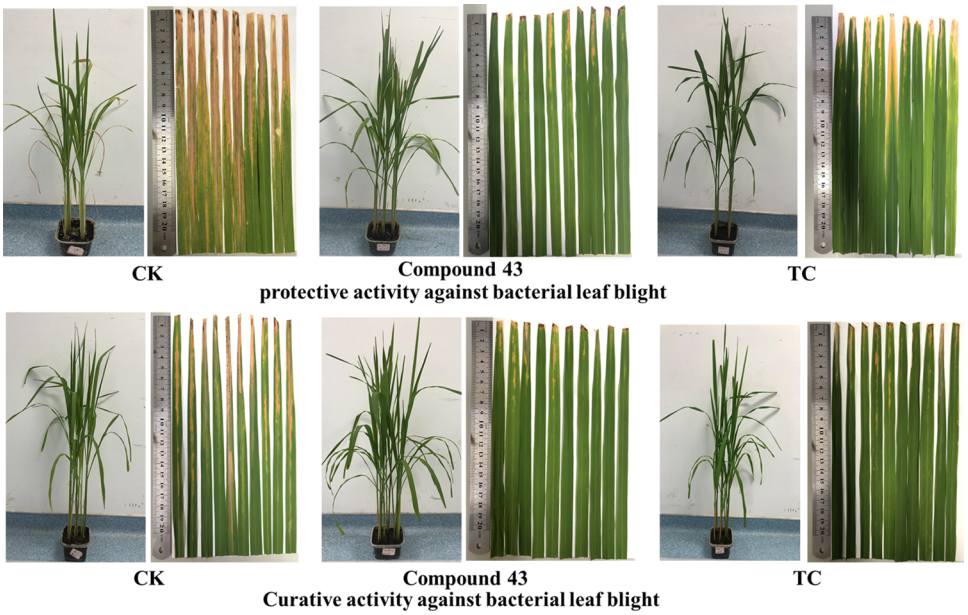

Figure 5. Protection and curative activities of compound **43** against rice bacterial leaf blight at 200 μg/mL.

Table 5. Protective and Curative Activities *In Vivo* of Compound 43 against Rice Bacterial Leaf Streak under Greenhouse Conditions at 200 μg/mL[a]

	14 days after spraying			
treatment	average lesion length (cm)	protective activity (%)[b]	average lesion length (cm)	curative activity (%)[b]
43	1.7	45.0 ± 2.8*a*	1.5	44.0 ± 1.8*b*
TC	1.9	38.0 ± 2.6*a*	1.7	41.2 ± 1.8*a*
CK	3.0		2.7	

[a]All results are expressed as mean ± SD. [b]Statistical analysis was performed by analysis of variance (ANOVA) in SPSS 22.0 software with equal variances assumed ($P > 0.05$). The different lowercase letters indicate curative activity with difference treatment groups at $P < 0.05$.

validation first, we then used non-cross-validation, and finally obtained the best 7 components, $q^2 = 0.705$, $r^2 = 0.982$, standard deviation SEE = 0.056, and the F-value = 127.121. At the same time, the relative contribution of the stereo and the electrostatic fields to the antibacterial effect of *Xoc* were 71.7 and 28.3%, respectively, indicating that the biological activity of the title compound is highly dependent on the interaction of the steric field. Through cross-validation and non-cross-validation, we established the CoMSIA model of the title compounds, where the cross-validation coefficient $r^2 = 0.627$, the cross-validated $q^2 = 0.918$, the optimal number of groups was 4, the standard deviation SEE = 0.113, and *F*-value = 40.152. The relative contributions of the H-donor, H-acceptor, hydrophobic, electrostatic, and steric fields to the antibacterial effect of *Xoc* were 6.4, 3.6, 35.7, 25.2, and 29.1%. Therefore, in CoMSIA, the hydrophobic effect, electrostatic effect, and steric effect play an important role in the anti-*Xoc* activity of title compounds. The correlation between the predicted and experimental pEC_{50} values of the CoMFA and CoMSIA models is shown in Figure 4. The predicted pEC_{50} values are in agreement with the experimental values within acceptable error limits for the reliability validation of the model and are shown in Table S1.

CoMFA Contour Map Analysis. As depicted in Figure 3a,b, the stereo field of CoMFA (Figure 3a) shows some yellow outlines adjacent to the R_2 position, as well as a small green patch adjacent to the 5th position of the indole ring, where the large population at the R_2 position inhibits antibacterial activity and the addition of a large chemical group at the 5th position of the indole ring contributes to the improvement of the anti-*Xoc* activity. These test results are consistent with the data found below: **1** (R_1: 5-H, R_2: $n = 5$, 16.6 μg/mL) > **3** (R_1: 5-H, R_2: $n = 7$,

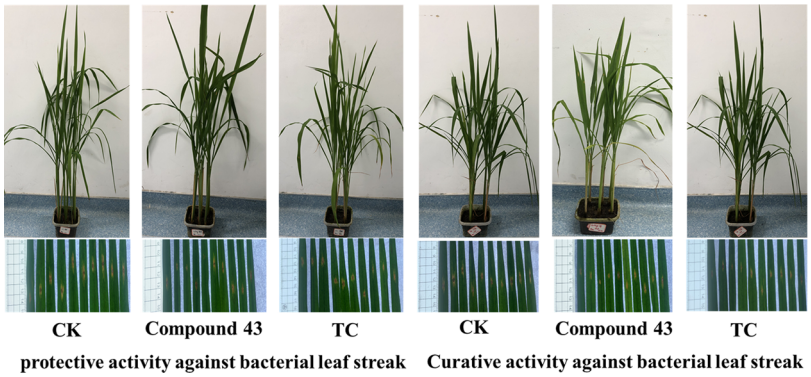

Figure 6. Protection and curative activities of compound **43** against rice bacterial leaf streak at 200 μg/mL.

https://doi.org/10.1021/acs.jafc.2c04213
J. Agric. Food Chem. 2022, 70, 12341−12354

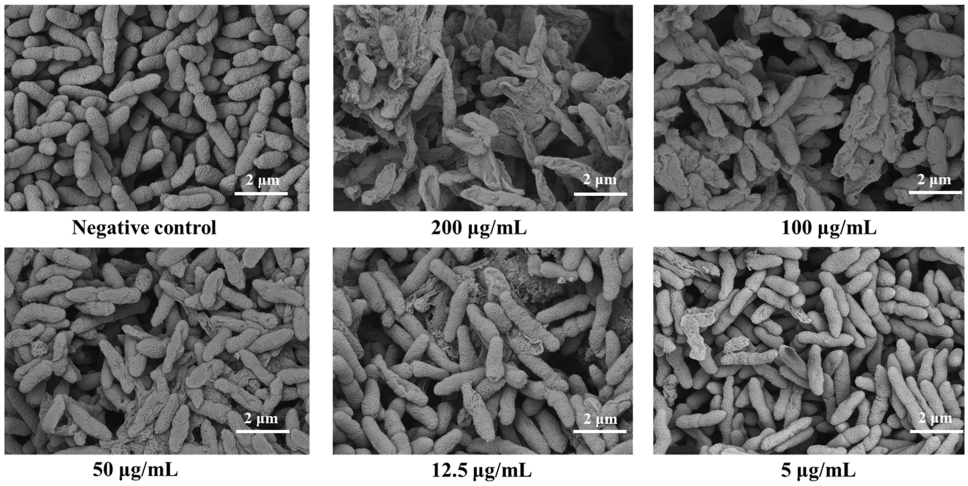

Figure 7. Effect of compound **43** on the cell morphology of *X. oryzae* pv. *oryzicola*.

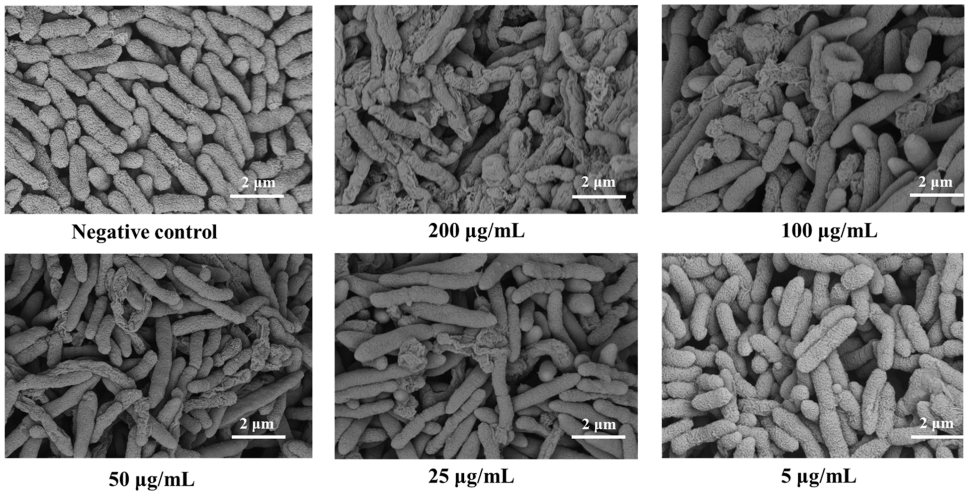

Figure 8. Effect of compound **43** on the cell morphology of *X. oryzae* pv. *oryzae*.

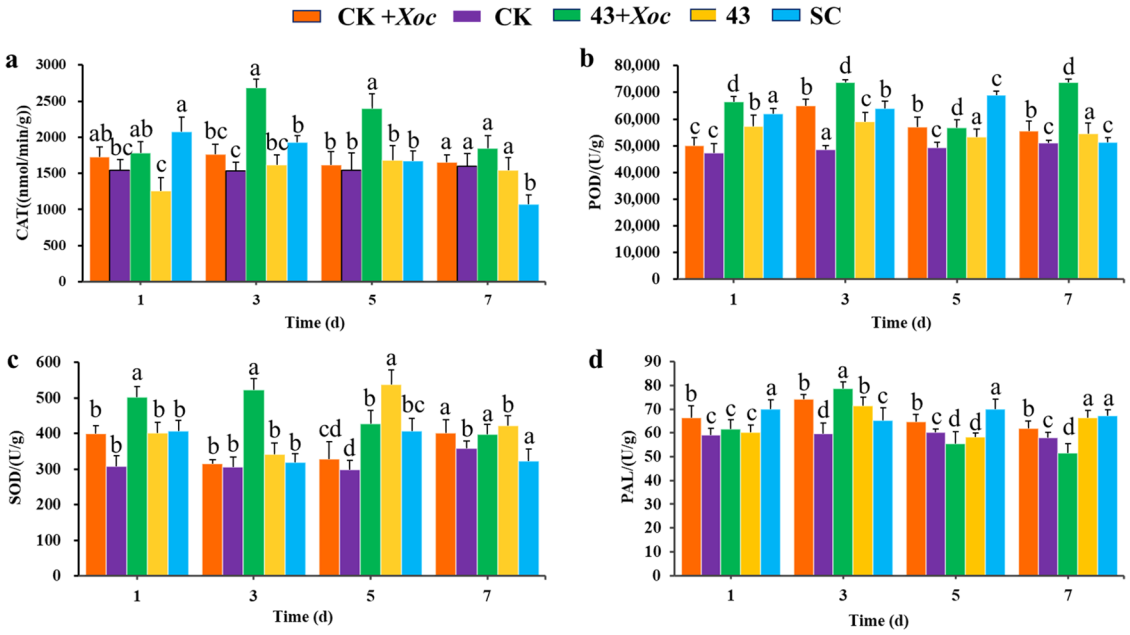

Figure 9. Effect of compound **43** on defense enzymes and chlorophyll in rice (a) catalase (CAT), (b) peroxidase (POD), (c) superoxide dismutase (SOD), and (d) phenylalanine ammonia-lyase (PAL).

https://doi.org/10.1021/acs.jafc.2c04213
J. Agric. Food Chem. 2022, 70, 12341−12354

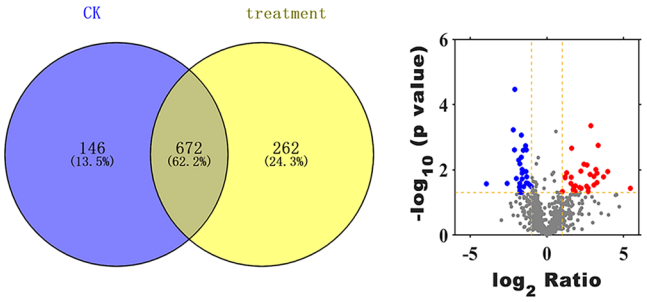

Figure 10. Venn diagram and volcano plot of proteins identified in the treatment and control groups. The red points are significantly upregulated proteins, while the blue points are significantly downregulated proteins.

23.8 μg/mL), **12** (R_1: 5-Br, R_2: n = 5, 19.6 μg/mL) > **13** (R_1: 5-Br, R_2: n = 6, 22.2 μg/mL), **31** (R_1: 5-Cl, R_2: n = 8, 5.8 μg/mL) > **23** (R_1: 5-H, R_2: n = 8, 21.1 μg/mL), **26** (R_1: 5-Cl, R_2: n = 1, 47.5 μg/mL) > **27** (R_1: 5-Cl, R_2: n = 4, 53.4 μg/mL). The electrostatic field diagram of the CoMFA model is demonstrated in Figure 3b. There are red modules adjacent to the indole ring, and the small space in the electron-withdrawing group in this region enhances the antibacterial activity. However, many red outlines and blue outlines were found near the pyridine ring, which almost surrounded the entire pyridine ring. This observation suggests that the introduction of a small electronegative group at an appropriate position in this region can enhance the inhibitory activity, as shown with the following results: **1** (R_1: 5-H, R_2: n = 5, 16.6 μg/mL) > **29** (R_1: 5-Cl, R_2: n = 6, 22.2 μg/mL), **31** (R_1: 5-Cl, R_2: n = 8, 5.8 μg/mL) > **35** (R_1: 5-Br, R_2: n = 8, 17.9 μg/mL).

CoMSIA Contour Map Analysis. The four types of contour maps of CoMSIA are indicated in Figure 3c–f. The stereo and electrostatic field equipotential diagrams of the CoMSIA model are shown in Figure 3c,d, respectively. The results of the stereo and electrostatic field equipotential diagrams of the CoMSIA model are consistent with those of the CoMFA model. Figure 3e,f exhibits the hydrogen-bond-acceptor contour maps of the CoMSIA model. There are yellow modules around the 5th position of the indole heterocycle and gray blocks around the pyridine ring, indicating that the introduction of a hydrophobic group at the 5th position of the indole heterocycle is beneficial to the improvement of antibacterial activity. When the pyridine ring is modified, the introduction of hydrophobic groups is not conducive to antibacterial activity. There is a magenta color block at the 2nd position of the indole ring, indicating that the introduction of a hydrogen-bond acceptor near the 2nd position of the indole ring can also improve the antibacterial biological activity as illustrated by comparing the EC_{50} of **32** (R_1: 5-Cl, R_2: n = 8, 4.9 μg/mL) > **4** (R_1: 5-H, R_2: n = 9, 41.9 μg/mL). From the above data analysis, under the conditions of the same number of carbon atoms of alkane, the 3rd position of the pyridine ring is modified and derived, and the antibacterial activity of the synthesized compound is better than that of the 4th position of the pyridine ring. Therefore, the modification at the 3rd position of the pyridine ring and the introduction of long-chain halogenated hydrocarbons are beneficial to the antibacterial activity, but the antibacterial activity gradually weakens after more than 12 carbon atoms.

Design and Synthesis of Compound 43. To further design and synthesize more active compounds based on the above 3D-QSAR model analysis, we know that the antibacterial activity of the title compounds is mainly affected by the hydrophobic effect, electrostatic effect, and steric effect. The 5th position of the indole ring was modified, and introduction of an electron-withdrawing group is beneficial to the improvement of

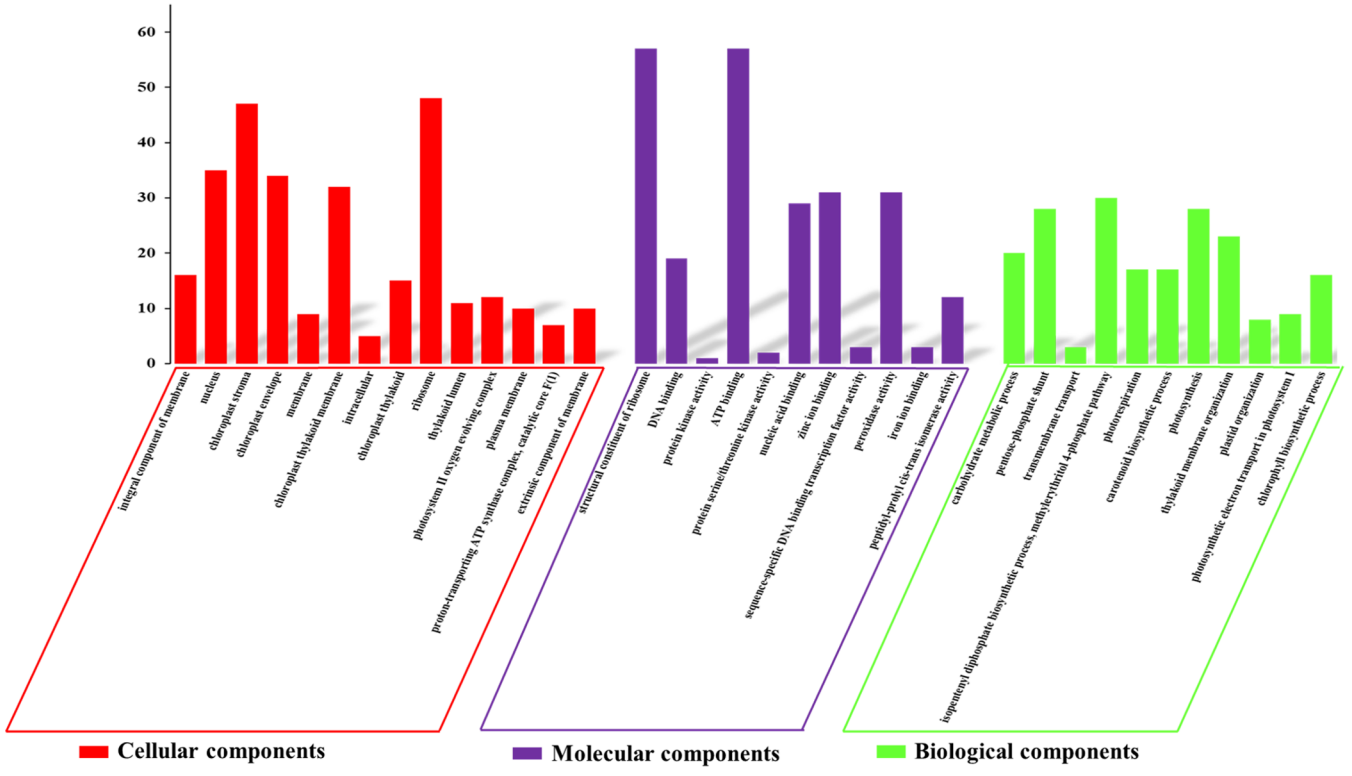

Figure 11. GO analysis of differentially expressed proteins between the control groups and compound **43** treatment groups.

https://doi.org/10.1021/acs.jafc.2c04213
J. Agric. Food Chem. 2022, 70, 12341−12354

antibacterial activity. The 3rd position of the pyridine ring was modified, and a long-chain alkyl group was introduced at the 3rd position, which was beneficial to the antibacterial activity of the synthesized title compound. Finally, the title compound **43** was designed and synthesized, and its antibacterial activity was evaluated *in vitro*. The biological test results showed that compound **43** had excellent antibacterial activity against *Xoc* and *Xoo*, with EC_{50} values of 1.9 and 1.0 μg/mL, respectively, which were better than those of the commercial drug TC (87.5 and 72.9 μg/mL, respectively). The above test results further verify the stability and prediction ability of 3D-QSAR.

***In Vivo* Antibacterial Activity.** Under the greenhouse conditions of 30 °C, the title compound **43** at a concentration of 200 μg/mL was used to determine the curative and protective effects of the title compound **43** on BLB *in vivo*, and the disease index was used to calculate the control effect. The results are displayed in Table 4 and Figure 5. The osmotic inoculation method was used to determine the title compound **43** at a concentration of 200 μg/mL, and the curative and protective effects of BLS on live potted plants were tested. The curative and protective activities of compound **43** against BLB were 39.3 and 42.0%, respectively, which were better than TC (37.0 and 38.6%). The length of the lesion was used to calculate the control effect. The results are indicated in Table 5 and Figure 6. The protective and curative activities of the title compound **43** against BLS were 45.0 and 44.0%, respectively, and the activity was better than that of the commercial drug TC (38.0 and 41.2%).

Morphological Changes. The morphological changes of *Xoc* and *Xoo* cells were observed with a scanning electron microscope Nova NanoSEM 450, as shown in Figures 7 and 8. SEM images show that compound **43** is concentration-dependent on the morphology of *Xoc* and *Xoo*. When the concentration of compound **43** was changed from 5 to 25 μg/mL, the morphology of compound **43** on *Xoc* and *Xoo* changed from a good shape to a partially corrugated or broken one. In the blank control group, the bacterial cell surface was intact and had no obvious change. This finding indicates that the title compound **43** has a strong interaction with these phytopathogens, and further increasing the drug concentration to 100 and 200 μg/mL resulted in the appearance of large amounts of bacterial debris and leak holes.

Increase the Activities of Plant Defense Enzymes. The activities of defense enzymes are closely related to the disease resistance of plants. The defense enzyme activities of the **43** + *Xoc* treatment group, compound **43** treatment, CK + *Xoc* treatment, CK treatment, and TC treatment were tested on rice. As an important endogenous active deaerator, CAT can remove hydrogen peroxide in plants, and hydrogen peroxide is one of the key enzymes in the biological defense system.[42] The test results of CAT activity are indicated in Figure 9**a**. The **43** + *Xoc* treatment group reached a peak CAT activity on the 3rd day after infection with bacterial *Xoc*, and the activity data reached 2685.2 nmol/min/g, while the CAT activity data of the **43** treatment, CK treatment, CK + *Xoc* treatment, and TC + *Xoc* treatment were 1617.4, 1533.2, 1763.2, and 1926.3 nmol/min/g, respectively. The CAT activity of the **43** + *Xoc* treatment was 1.7, 1.8, 0.9, and 1.4 times those of the title compound **43** treatment, CK treatment, CK + *Xoc* treatment, and TC + *Xoc* treatment, respectively. POD can remove H_2O_2 and generate lignin through a series of changes, which enhances the plant's resistance to external damage and pathogen infection. SOD enzymes can destroy superoxide anion free radicals, generate H_2O_2 and O_2, and protect plants from free radical damage. As shown in Figure 9b,b, the results showed that the activities of POD and SOD in rice treated with compound **43** showed a trend of increasing first and then decreasing. The **43** + *Xoc* treatment had the highest POD activity on the 7th day after bacterial *Xoc* infection; the activity data reached 73828.7 U/g, while the POD activity data of the compound **43** treatment, CK treatment, CK + *Xoc* treatment, and TC + *Xoc* treatment were 54487.3, 51118.0, 55634.0, and 51224.7 U/g, respectively. The POD activity of the **43** + *Xoc* treatment was 1.4, 1.4, 1.3, and 1.4 times those of the compound **43** treatment, CK treatment, CK +*Xoc* treatment, and TC + *Xoc* treatment, respectively. The **43** + *Xoc* treatment had the highest SOD activity on the 3rd day after bacterial infection; the activity data reached 523.3 U/g, while the SOD activity data of the compound **43** treatment, CK treatment, CK + *Xoc* treatment, and TC + *Xoc* treatment were 340.9, 306.5, 314.8, and 319.1 U/g, respectively. The SOD activity of the **43** + *Xoc* treatment was 1.5, 1.7, 1.7, and 1.6 times those of the title compound **43** treatment, CK treatment, CK + *Xoc* treatment, and TC + *Xoc* treatment, respectively. As depicted in Figure 9d, the activity of PAL in rice treated with compound **43** showed a trend of increase at the first and then decreased, reaching a peak on the 3rd day. The activity data reached 78.8 U/g, while the PAL activity data of the compound **43** treatment, CK treatment, CK+*Xoc* treatment, and TC+*Xoc* treatment were 71.5, 59.6, 74.2, and 65.4 U/g, respectively. The PAL activity of the **43** + *Xoc* treatment was 1.1, 1.3, 1.7, and 1.2 times those of the title compound **43** treatment, CK treatment, CK+*Xoc* treatment, and TC+*Xoc* treatment, respectively. It has been reported in the literature that isoflavone phytoalexins and flavonoid pigments are involved in plant defense against pathogens, and these two species can be synthesized by PAL catalysis.[44] Compared with CK+*Xoc* treatment and CK treatment, the PAL activity of **43** + *Xoc* treatment was not significantly increased. Therefore, the title compound **43** might enhance rice resistance by increasing CAT, SOD, and POD activities in rice.

Proteomics Analysis. A total of 1080 proteins were identified in the "Fengyouxiangzhan" rice in the compound **43** + *Xoc* treatment group and the rice in the blank control group **CK** + *Xoc*, of which 818 proteins were identified in the control rice **CK** + *Xoc*, and 146 were specifically expressed, and 934 proteins were identified and 262 were specifically expressed in the rice in the compound **43** + *Xoc* treatment group. At the same time, a total of 934 proteins were differentially expressed in response to the **43** + *Xoc* stimulation of rice in the treatment group (Figure 10). Among the 934 proteins, 175 and 294 proteins were downregulated (blue points) and upregulated (red points), respectively.

Biofunctional Analysis. According to the GO enrichment analysis of the differentially expressed proteins of compound **43** *vs* CK, Go analysis is divided into three categories: BPs, CCs, and MFs. As depicted in Figure 11, the results by GO enrichment indicated that most DEPs were located in CCs, such as the nucleus, intracellular, thylakoid, ribosomes, chloroplast stroma, thylakoid lumen, and photosystem II oxygen-evolving complex. MF analysis indicated that the differentially expressed proteins were associated with DNA binding, peroxidase activity, iron ion binding, ATP binding, and so on. In the BP analysis, varying levels of proteins were involved in the methyl erythritol 4-phosphate pathway, photorespiration, transmembrane transport, plastid organization, thylakoid membrane organization, chlorophyll biosynthetic process, etc. These results indicated that the title compound **43** might

https://doi.org/10.1021/acs.jafc.2c04213
J. Agric. Food Chem. 2022, 70, 12341−12354

modulate and interfere with many aspects of pathogenic *Xoc* physiological processes and plant defense processes, thereby increasing disease resistance in rice.

Functional Classification of KEGG. To further explore and study the disease resistance pathway triggered by the title compound **43** after stimulating rice, we performed KEGG analysis on the experimental data of the *Xoc* group and the *Xoc* + **43** group. KEGG analysis revealed four significantly enriched pathways in DEPs, including glycolysis/gluconeogenesis, oxidative phosphorylation, citrate cycle (TCA cycle), and pyruvate metabolism. These significantly enriched pathways are mainly related to the energy metabolism pathways of plants,[45] and this shows that compound **43** may regulate the conversion of glycolysis in rice to produce the intermediate product pyruvate,[46] which undergoes a deacidification reaction under aerobic conditions to generate acetyl-CoA and then enters the citric acid cycle, where acetic acid and water are consumed, NAD^+ is reduced to NADH, and carbon dioxide is released. Consequently, NADH produced during the citric acid cycle is fed into the oxidative phosphorylation pathway (electron transport).[47] The end result of these two closely related pathways is that nutrients are oxidized to produce usable chemical energy in the form of ATP to supply plants, thereby increasing plant disease resistance.

In summary, we have successfully introduced active pyridinium moieties into indole compounds and synthesized a series of novel indole derivatives. Among them, the antibacterial test results showed that compounds **31**, **32**, **34**, and **35** could severely inhibit both *Xoc* and *Xoo* plant pathogens with EC_{50} values of 5.8, 4.9, 9.6, 17.9 and 5.6, 5.5, 5.5, 4.8 μg/mL, respectively. To discover higher activity title compounds, we also constructed 3D-QSAR models based on the *Xoc* antibacterial activities of the title compounds. The title compound **43** was subsequently designed and synthesized, and the *in vivo* study on plant pathogens further verified that the title compound **43** has the potential to replace the current commercial antibacterial agents. Quantitative proteomic analysis revealed that 934 proteins (175 and 294 proteins were downregulated and upregulated, respectively) were observed to be differentially expressed in response to stimulation with the title compound **43**, suggesting that this kind of compound might modulate and interfere with the physiological processes and functions of pathogenic bacteria. This result was further confirmed by defense enzyme activity tests and scanning electron microscopy images. Therefore, considering the simplicity of the title compound structures, easy synthetic process, and highly efficient bioactivity, novel indole derivatives containing pyridinium moieties can serve as lead structures for the discovery of antibacterial agents. We expect our study to bring significant meaning to the discovery and design of novel green pesticides based on natural substances.

■ ASSOCIATED CONTENT

Supporting Information

The Supporting Information is available free of charge at https://pubs.acs.org/doi/10.1021/acs.jafc.2c04213.

Physical analysis; high-resolution mass spectrum (HRMS); and NMR spectra of compounds **1**−**43** can be found (PDF)

All identified proteins (XLSX)

■ AUTHOR INFORMATION

Corresponding Author

Runjiang Song − *State Key Laboratory Breeding Base of Green Pesticide and Agricultural Bioengineering, Key Laboratory of Green Pesticide and Agricultural Bioengineering, Ministry of Education, Research and Development Center for Fine Chemicals, Guizhou University, Guiyang 550025, China;* orcid.org/0000-0003-2502-778X; Phone: 86−851−8829−2170; Email: songrj@gzu.edu.cn; Fax: 86−851−83622211

Authors

Hongde Li − *State Key Laboratory Breeding Base of Green Pesticide and Agricultural Bioengineering, Key Laboratory of Green Pesticide and Agricultural Bioengineering, Ministry of Education, Research and Development Center for Fine Chemicals, Guizhou University, Guiyang 550025, China;* orcid.org/0000-0002-5888-6188

Shang Wu − *State Key Laboratory Breeding Base of Green Pesticide and Agricultural Bioengineering, Key Laboratory of Green Pesticide and Agricultural Bioengineering, Ministry of Education, Research and Development Center for Fine Chemicals, Guizhou University, Guiyang 550025, China;* orcid.org/0000-0002-2220-7518

Xiong Yang − *State Key Laboratory Breeding Base of Green Pesticide and Agricultural Bioengineering, Key Laboratory of Green Pesticide and Agricultural Bioengineering, Ministry of Education, Research and Development Center for Fine Chemicals, Guizhou University, Guiyang 550025, China;* orcid.org/0000-0002-0656-5809

Hongfu He − *State Key Laboratory Breeding Base of Green Pesticide and Agricultural Bioengineering, Key Laboratory of Green Pesticide and Agricultural Bioengineering, Ministry of Education, Research and Development Center for Fine Chemicals, Guizhou University, Guiyang 550025, China;* orcid.org/0000-0002-6745-1936

Zengxue Wu − *State Key Laboratory Breeding Base of Green Pesticide and Agricultural Bioengineering, Key Laboratory of Green Pesticide and Agricultural Bioengineering, Ministry of Education, Research and Development Center for Fine Chemicals, Guizhou University, Guiyang 550025, China;* orcid.org/0000-0003-3629-7259

Baoan Song − *State Key Laboratory Breeding Base of Green Pesticide and Agricultural Bioengineering, Key Laboratory of Green Pesticide and Agricultural Bioengineering, Ministry of Education, Research and Development Center for Fine Chemicals, Guizhou University, Guiyang 550025, China;* orcid.org/0000-0002-4237-6167

Complete contact information is available at: https://pubs.acs.org/10.1021/acs.jafc.2c04213

Notes

The authors declare no competing financial interest.

■ ACKNOWLEDGMENTS

The authors are grateful to the National Key Research Development Program of China (2018YFD0200100) for supporting the project.

■ ABBREVIATIONS USED

Xoc, *Xanthomonas oryzae* pv. *oryzicola*; *Xoo*, *Xanthomonas oryzae* pv. *oryzae*; BLS, rice bacterial leaf streak; BLB, rice bacterial

blight; EC_{50}, half-maximal effective concentration; TC, thiodiazole copper; DEPs, differentially expressed proteins; GO, Gene Ontology; BPs, biological processes; CCs, cellular components; MFs, molecular functions; KEGG, Kyoto Encyclopedia of Genes and Genomes; PBS, phosphate-buffered saline; SOD, superoxide dismutase; POD, peroxidase; PAL, phenylalanine ammonia-lyase; CAT, catalase

REFERENCES

(1) Jiang, N.; Yan, J.; Liang, Y. L.; Shi, Y.; He, Z. Z.; He, Z.; Wu, Y. T.; Wu, Y.; Zeng, Q.; Zeng, Q.; Liu, X. J.; Liu, X.; Peng, J. H. Resistance genes and their interactions with bacterial blight/leaf streak pathogens (*Xanthomonas oryzae*) in rice (*Oryza sativa* L.)-an updated review. *Rice* **2020**, *13*, No. 3.

(2) Mansfield, J.; Genin, S.; Magori, S.; Citovsky, V.; Sriariyanum, M.; Ronald, P.; Dow, M.; Verdier, V.; Beer, S. V.; Machado, M. A.; Toth, I.; Salmond, G.; Foster, G. D. Top 10 plant pathogenic bacteria in molecular plant pathology. *Mol. Plant Pathol.* **2012**, *13*, 614−629.

(3) Cai, L. L.; Cao, Y. Y.; Xu, Z. Y.; Ma, W. X.; Zakria, M.; Zou, L. F.; Cheng, Z. Q.; Chen, G. Y. A transcription activator-like effector *Tal7* of *Xanthomonas oryzae* pv. *oryzicola* activates rice gene *Os09g29100* to suppress rice immunity. *Sci. Rep.* **2017**, *7*, No. 5089.

(4) Khan, M. I. R.; Palakolanu, S. R.; Chopra, P.; Rajurkar, A. B.; Gupta, R.; Iqbal, N.; Maheshwari, C. Improving drought tolerance in rice: ensuring food security through multi-dimensional approaches. *Physiol. Plant.* **2021**, *172*, 645−668.

(5) Li, P.; Shi, L.; Yang, X.; Yang, L.; Chen, X. W.; Wu, F.; Shi, Q. C.; Xu, W. M.; He, M.; Hu, D. Y.; Song, B. A. Design, synthesis, and antibacterial activity against rice bacterial leaf blight and leaf streak of -2,5-substituted-1,3,4-oxadiazole/thiadiazole sulfone derivative. *Bioorg. Med. Chem. Lett.* **2014**, *24*, 1677−1680.

(6) Iacobellis, N. S.; Lo, C. P.; Capasso, F.; Senatore, F. Antibacterial activity of *Cuminum cyminum* L. and *Carum carvi* L. essential oils. *J. Agric. Food Chem.* **2005**, *53*, 57−61.

(7) Sundin, G. W.; Castiblanco, L. F.; Yuan, X. C.; Zeng, Q.; Yang, C. H. Bacterial disease management: challenges, experience, innovation and future prospects. *Mol. Plant Pathol.* **2016**, *17*, 1506−1518.

(8) Wightwick, A. M.; Mollah, M. R.; Partington, D. L.; Allinson, G. Copper fungicide residues in Australian vineyard soils. *J. Agric. Food Chem.* **2008**, *56*, 2457−2464.

(9) Stockwell, V. O.; Duffy, D. Use of antibiotics in plant agriculture. *Rev. Sci. Tech.* **2012**, *31*, 199−210.

(10) Ferrer, L.; Mindt, M.; Suarez-Diez, M.; Jilg, T.; Zagorščak, M.; Lee, J. H.; Gruden, K.; Wendisch, V. F.; Cankar, K. Fermentative indole production via bacterial tryptophan synthase alpha subunit and plantindole-3-glycerol phosphate lyase enzymes. *J. Agric. Food Chem.* **2022**, *70*, 5634−5645.

(11) Salimova, E. V.; Magafurova, A. A.; Tret'Yakova, E. V.; Kukovinets, O. S.; Parfenova, L. V. Indole derivatives of fusidane triterpenoids: synthesis and the antibacterial activity. *Chem. Heterocycl. Compd.* **2020**, *56*, 800−804.

(12) Wu, S. Q.; Li, X. Q.; Meng, J.; Gan, Y. Y.; Tian, K.; Wan, Z. C.; Ouyang, G. P. Synthesis and antibacterial activity of 2-morpholino-1-propyl-1*H*-indole-3-substituted acylhydrazone derivatives. *Chin. J. Org. Chem.* **2018**, *38*, 1447−1453.

(13) Li, X. Q.; Gan, Y. Y.; Meng, J.; Li, W.; Chen, J.; Qi, Y. Y.; Tian, K.; Ouyang, G. P.; Wang, Z. C. Synthesis and antimicrobial activities of novel quinazolinone acylhydrazone derivatives containing the indole moiety. *J. Heterocycl. Chem.* **2018**, *55*, 1382−1390.

(14) Liu, H. B.; Lauro, G.; O'Connor, R. D.; Lohith, K.; Kelly, M.; Colin, P.; Bifulco, G.; Bewley, C. A. Tulongicin, an antibacterial tri-indole alkaloid from a deep-water *Topsentia sp. Sponge*. *J. Nat. Prod.* **2017**, *80*, 2556−2560.

(15) Yu, H. F.; Huang, W. Y.; Ding, C. F.; Wei, X.; Zhang, L. C.; Qin, X. J.; Ma, H. X.; Yang, Z. F.; Liu, Y. P.; Zhang, R. P.; Wang, X. H.; Luo, X. D. Cage-like monoterpenoid indole alkaloids with antimicrobial activity from *Alstonia scholaris*. *Tetrahedron Lett.* **2018**, *59*, 2975−2978.

(16) Qin, X. J.; Zhao, Y. L.; Lunga, P. K.; Yang, X. W.; Song, C. W.; Cheng, G. G.; Liu, L.; Chen, Y. Y.; Liu, Y. P.; Luo, X. D. Indole alkaloids with antibacterial activity from aqueous fraction of *Alstonia scholaris*. *Tetrahedron* **2015**, *71*, 4372−4378.

(17) Shah, R. J.; Modi, N. R.; Patel, M. J.; Patel, L. J.; Chauhan, B. F.; Patel, M. M. Design, synthesis and *in vitro* antibacterial and antifungal activities of some novel spiro[azetidine-2,3′-indole]-2,4(1′*H*)-dione. *Med. Chem. Res.* **2011**, *20*, 587−594.

(18) Deokar, H.; Chaskar, J.; Chaskar, A. Synthesis and antimicrobial activity evaluation of novel oxadiazino/thiadiazino-indole and oxadiazole/thiadiazole derivatives of 2-oxo-2*H*-benzopyran. *J. Heterocyclic. Chem.* **2014**, *51*, 719−725.

(19) Saundane, A. R.; Walmik, P.; Yarlakatti, M.; Katkar, V.; Verma, V. A. Synthesis and biological activities of some new annulated pyrazolopyranopyrimidines and their derivatives containing indole nucleus. *J. Heterocyclic. Chem.* **2014**, *51*, 303−314.

(20) Mane, Y. D.; Sarnikar, Y. P.; Surwase, S. M.; Biradar, D. O.; Gorepatil, P. B.; Shinde, V. S.; Khade, B. C. Design, synthesis, and antimicrobial activity of novel 5-substituted indole-2-carboxamide derivatives. *Res. Chem. Intermed.* **2016**, *43*, 1−23.

(21) Song, F.; Bian, Y. Q.; Liu, J.; Li, Z. H.; Zhao, L.; Fang, J. M.; Lai, Y. H.; Zhou, M. Indole alkaloids, synthetic dimers and hybrids with potential in vivo anticancer activity. *Curr. Top. Med. Chem.* **2021**, *21*, 377−403.

(22) Zhou, J.; Feng, J. H.; Fang, L. A novel monoterpenoid indole alkaloid with anticancer activity from *Melodinus khasianus*. *Bioorg. Med. Chem. Lett.* **2017**, *27*, 893−896.

(23) Song, H. J.; Liu, Y. X.; Liu, Y. X.; Huang, Y. Q.; Li, Y. Q.; Wang, Q. M. Design, synthesis, anti-TMV, fungicidal, and insecticidal activity evaluation of 1,2,3,4-tetrahydro-*β*-carboline-3-carboxylic acid derivatives based on virus inhibitors of plant sources. *Bioorg. Med. Chem. Lett.* **2014**, *24*, 5228−5233.

(24) Liu, Y. X.; Song, H. J.; Huang, Y. Q.; Li, J. R.; Zhao, S.; Song, Y. C.; Yang, P. W.; Xiao, Z. X.; Liu, Y. X.; Li, Y. Q.; Shang, H.; Wang, Q. M. Design, synthesis, and antiviral, fungicidal, and insecticidal activities of tetrahydro-*β*-carboline-3-carbohydrazide derivatives. *J. Agric. Food Chem.* **2014**, *62*, 9987−9999.

(25) Ji, X. F.; Wang, Z. W.; Dong, J.; Liu, Y. X.; Lu, A. D.; Wang, Q. M. Discovery of topsentin alkaloids and their derivatives as novel antiviral and anti-phytopathogenic fungus agents. *J. Agric. Food Chem.* **2016**, *64*, 9143−9151.

(26) Song, J.; Chen, D. F.; Gong, L. Z. Recent progress in organocatalytic asymmetric total syntheses of complex indole alkaloids. *Natl. Sci. Rev.* **2017**, *4*, 381−396.

(27) Nemoto, T.; Harada, S.; Nakajima, M. Synthetic methods for 3,4-fused tricyclic indoles via indole ring formation. *Asian J. Org. Chem.* **2018**, *7*, 1730−1742.

(28) Wang, P. Y.; Gao, M. N.; Zhou, L.; Wu, Z. B.; Hu, D. Y.; Hu, J.; Yang, S. Synthesis and antibacterial activity of pyridinium-tailored aromatic amphiphiles. *Bioorg. Med. Chem. Lett.* **2016**, *26*, 1136−1139.

(29) Wang, P. Y.; Zhou, L.; Zhou, J.; Wu, Z. B.; Xue, W.; Song, B. A.; Yang, S. Synthesis and antibacterial activity of pyridinium-tailored 2,5-substituted-1,3,4-oxadiazole thioether/sulfoxide/sulfone derivatives. *Bioorg. Med. Chem. Lett.* **2016**, *26*, 1214−1217.

(30) Wang, P. Y.; Wang, M. W.; Zeng, D.; Xiang, M.; Rao, J. R.; Liu, Q. Q.; Liu, L. W.; Wu, Z. B.; Li, Z.; Song, B. A.; Yang, S. Rational optimization and action mechanism of novel imidazole (or imidazolium)-labeled 1,3,4-oxadiazole thioethers as promising antibacterial agents against plant bacterial diseases. *J. Agric. Food Chem.* **2019**, *67*, 3535−3545.

(31) Li, P.; Hu, D. Y.; Xie, D. D.; Chen, J. X.; Jin, L. H.; Song, B. A. Design, synthesis, and evaluation of new sulfone derivatives containing a 1,3,4-oxadiazole moiety as active antibacterial agents. *J. Agric. Food Chem.* **2018**, *66*, 3093−3100.

(32) Sun, N. B.; Shi, Y. X.; Liu, X. H.; Ma, Y.; Tan, C. X.; Weng, J. Q.; Jin, J. Z.; Li, B. J. Design, synthesis, antifungal activities and 3D-QSAR of new *N*,*N*′-diacylhydrazines containing 2,4-dichlorophenoxy moiety. *Int. J. Mol. Sci.* **2013**, *14*, 21741−21756.

https://doi.org/10.1021/acs.jafc.2c04213
J. Agric. Food Chem. 2022, 70, 12341−12354

(33) Zheng, X. M.; Li, Z.; Wang, Y. L.; Chen, W. D.; Huang, Q. C.; Liu, C. X.; Song, G. H. Syntheses and insecticidal activities of novel 2,5-disubstituted 1,3,4-oxadiazoles. *J. Fluor. Chem.* **2003**, *123*, 163−169.
(34) Zhang, X. N.; Breslav, M.; Grimm, J.; Guan, K. L.; Huang, A. H.; Liu, F. Q.; Maryanoff, C. A.; Palmer, D.; Patel, M.; Qian, Y.; Shaw, C.; Sorgi, K.; Stefanick, S.; Xu, D. W. A new procedure for preparation of carboxylic acid hydrazides. *J. Org. Chem.* **2002**, *67*, 9471−9474.
(35) Wu, S. K.; Shi, J.; Chen, J. X.; Hu, D. Y.; Zang, L. S.; Song, B. A. Synthesis, antibacterial activity, and mechanisms of novel 6-sulfonyl-1,2,4-triazolo[3,4-b][1,3, 4]thiadiazole derivatives. *J. Agric. Food Chem.* **2021**, *69*, 4645−4654.
(36) Chen, J. X.; Luo, Y. Q.; Wei, C. Q.; Wu, S. K.; Wu, R.; Wang, S. B.; Hu, D. Y.; Song, B. A. Novel sulfone derivatives containing a 1,3,4-oxadiazole moiety: design and synthesis based on the 3D-QSAR model as potential antibacterial agent. *Pest Manage. Sci.* **2020**, *76*, 3188−3198.
(37) Xu, W.-M.; Han, F.-F.; He, M.; Hu, D.-Y.; He, J.; Yang, S.; Song, B.-A. Inhibition of tobacco bacterial wilt with sulfone derivatives containing an 1,3,4-oxadiazole moiety. *J. Agric. Food Chem.* **2012**, *60*, 1036−1041.
(38) Wang, S. B.; Gan, X. H.; Wang, Y. J.; Li, S. Y.; Yi, C. F.; Chen, J. X.; He, F. C.; Yang, Y. Y.; Hu, D. Y.; Song, B. A. Novel 1,3,4-oxadiazole derivatives containing a cinnamic acid moiety as potential bactericide for rice bacterial diseases. *Int. J. Mol. Sci.* **2019**, *20*, 1020−1037.
(39) Kvasko, O. Y.; Matvieieva, N. A. Increasing of antioxidant and superoxide dismutase activity in chicory transgenic plants. *Biopolym. Cell.* **2013**, *29*, 163−166.
(40) Chen, Q.; Man, H.; Zhu, L.; Guo, Z. J.; Wang, X. L.; Tu, J. P.; Jin, G.; Lou, J.; Zhang, L.; Ci, L. J. Enhanced plant antioxidant capacity and biodegradation of phenol by immobilizing peroxidase on amphoteric nitrogen-doped carbon dots. *Catal. Commun.* **2019**, *134*, No. 105847.
(41) Ertani, A.; Pizzeghello, D.; Francioso, O.; Tinti, A.; Nardi, S. Biological activity of vegetal extracts containing phenols on plant metabolism. *Molecules* **2016**, *21*, No. 205.
(42) Chen, F.; Wang, M.; Zheng, Y.; Luo, J.; Yang, X.; Wang, X. Quantitative changes of plant defense enzymes and phytohormone in biocontrol of cucumber fusarium wilt by bacillus subtilis B579. *World J. Microbiol. Biotechnol.* **2010**, *26*, 675−684.
(43) Yu, L.; Wang, W. L.; Zeng, S.; Chen, Z.; Yang, A. M.; Shi, J.; Zhao, X. Z.; Song, B. A. Label-free quantitative proteomics analysis of cytosinpeptidemycin responses in southern rice black-streaked dwarf virus-infected rice. *Pestic. Biochem. Physiol.* **2018**, *147*, 20−26.
(44) Dixon, R. A.; Achnine, L.; Kota, P.; Liu, C.-J.; Reddy, M. S. S.; Wang, L. J. The phenylpropanoid pathway and plant defence-a genomics perspective. *Mol. Plant Pathol.* **2002**, *3*, 371−390.
(45) Bailey-Serres, J.; Fukao, T.; Gibbs, D. J.; Holdsworth, M. J.; Lee, S. C.; Licausi, F.; Perata, P.; Voesenek, L. A. C. J.; van Dongen, J. T. Making sense of low oxygen sensing. *Trends Plant. Sci.* **2012**, *17*, 129−138.
(46) Serafini, A.; Tan, L.; Horswell, S.; Howell, S.; Greenwood, D. J.; Hunt, D. M.; Phan, M. D.; Schembri, M.; Monteleone, M.; Montague, C. R.; Britton, W.; Garza-Garcia, A.; Snijders, A. P.; VanderVen, B.; Gutierrez, M. G.; West, N. P.; de Carvalho, L. P. S. *Mycobacterium tuberculosis* requires glyoxylate shunt and reverse methylcitrate cycle for lactate and pyruvate metabolism. *Mol. Microbiol.* **2019**, *112*, 1284−1307.
(47) Wilson, D. F.; Matschinsky, F. M. Metabolic homeostasis: Oxidative phosphorylation and the metabolic requirements of higher plants and animals. *J. Appl. Physiol.* **2018**, *125*, 1183−1192.

https://doi.org/10.1021/acs.jafc.2c04213
J. Agric. Food Chem. 2022, 70, 12341−12354